

Electronic Supplementary Information

Unusual Design Strategy of Stable and Soluble High-Molecular-Weight Copper(I) arylacetylide Polymers

Li Jiang, Jiangtao Jia, Yongchang Zhai, Zhiqiang Zhao, Yu Chen, Fengchao Cui,[†] Zheng Bian,^{*} Hongkun Tian, Chuanqiang Kang, Lianxun Gao, Mohamed Eddaoudi, and Guangshan Zhu

1. Materials and methods

All reagents were obtained from commercial suppliers and were used without further purification with exception of CHCl_3 . CHCl_3 was purified by distillation according to standard methods. Elemental analyses of complexes were measured by Elementarvario EL cube and Thermo Scientific XseriesII ICP-MS. IR spectra (KBr) were recorded on a Bruker Vertex70 Win-IR instrument. Raman spectra were recorded on a Thermo Nicolet FT-Raman 960. The X-ray photoelectron spectra (XPS) were measured on a Thermo Escalab 250 using Al Ka ($h\nu = 1486.6$ eV) radiation at 2×10^{-6} Pa, and charging effect calibrated by the C1s peak at 284.8 eV. The number-average molecular weights and weight-average molecular weights of complexes were measured at 25 °C by a gel permeation chromatograph (GPC) equipped with a Waters 1515 HPLC pump, column (HT4 THF) and a Waters 2414 refractive index detector. CHCl_3 was used as eluent at flow rate of 1.0 mL min^{-1} ($c = 0.5$ mg mL^{-1} , CHCl_3). Thermogravimetric analyses were obtained on Pyris Diamond TG/DAT thermal analyser in air and N_2 with 10 °C \cdot min^{-1} heating rate. Differential scanning calorimetry (DSC) experiments were carried out on PerkinElmer DSC 7 at 10 °C min^{-1} . UV-Vis absorption spectra were performed on a SHIMADZU UV-2550 ultraviolet spectrophotometer. Cyclic voltammetry (CV) was carried out with a CHI660E electrochemical workstation at a scan rate of 0.05 V s^{-1} . Polymer film on glassy carbon electrode used as the working electrode, a saturated calomel electrode (SCE) as the reference electrode, a Pt sheet as the counter electrode, and 0.1 M tetrabutylammonium perchlorate acetonitrile solution as the electrolyte. Solution was bubbled into N_2 for 20 min to remove O_2 . Photoluminescence spectra of complexes ($c = 0.1$ mg mL^{-1} , CHCl_3) were recorded by PerkinElmer Fluorescence Spectrometer FL6500. Time-resolved photoluminescence decay spectra of complexes were monitored on FISP920 Edinburgh fluorescence spectrometer. The emission quantum yields of complexes of 0.5 mg/mL in CHCl_3 were obtained on FIS1000 Edinburgh fluorescence spectrometer (excitation wavelength, 447 nm). The morphology of complexes film spin-coated on silicon slice was examined on a scanning electron microscope (HITACHI SU8010). TEM images were obtained by using a JEM-1011 electron microscope operating at an acceleration voltage of 100 kV. A carbon-coated copper grid was quickly put into the solution for less than 1 s and dried in air at room temperature. PXRD patterns were recorded with a Bruker D8 Advance diffractometer with CuK radiation ($\lambda = 0.154$ nm). The photoconductive property was measured using a Keysight B1500A analyzer. The light source for characterization was provided from LL470G-2500 470 nm fiber-optic laser with FY2300A frequency meter which gives pulse square wave. The thicknesses of thin films were measured by KLA Tencor P-7 stylus profilometer. The deposition of Au on film was carried out using Shenyang QiHui Z300C Vacuum system. The most stable geometry optimization accumulation pattern of complex $2 \cdot \text{Cu}$ by Materials Studio.

PXRD analysis: We firstly tried the direct structure solution from the PXRD data by EXPO 2014 software, however, due to the relatively weak diffraction intensity, we can't get all the structure information. By the same software, we can get the unit cell which was indexed using DICOL91 method. According to the elemental analysis and spectrum information, we observed this new material may have the similar assembling style like the reported structure by Che et. al.¹ The structure of $2 \cdot \text{Cu}$ was then modeled based on this published crystal structure with a space group of P21 and the unit cell obtained above. The geometry of the simulated structure was optimized by the force field in Material Studio software with a fixed unit cell. Then we used this optimized structure as the primary model and utilized the simulated annealing module in EXPO 2014 software to find the right position of the atoms. However, we observed that the solved structure after simulated annealing still have some unreasonable bonds. And again using Material Studio software we manually fixed the bond lengths and angles to get a relatively reasonable structure. The final structure was refined by a Pawley method in EXPO 2014 software giving good fitting factors of Rwp (4.97%) and Rp (3.34%).

All calculations were carried out using the density functional theory (DFT) with the ω B97XD functional³ including an attractive dispersion term as implemented in the Gaussian 16 program.⁴ All

geometry structures were optimized at the ω B97XD/6-31G(d,p) level of theory. The solvent effects were considered by the CPCM model⁵⁻⁶ with chloroform. Partial charges of atoms were produced by fitting to the restrained electrostatic potential calculated with 6-311++G(2d,2p) basis set, according to Merz-Singh-Kollman scheme.⁷⁻⁸

2. Synthesis of complexes and fabrication of devices

Synthesis of complexes

Ligands **1-8** were synthesized according to the references.^{2,9}

General synthetic method of complexes: Ligand, $\text{CuBF}_4(\text{CH}_3\text{CN})_4$ and solvent were added into a round-bottomed flask. Then the mixture was stirred for a period of time at room temperature. After adding base, the mixture was stirred for a period of time again. The soluble product was obtained by pouring viscous solution into methanol slowly under violent stirring. The insoluble product was obtained by filtering and washing the precipitate.

Fabrication of devices

The complexes solutions of different concentrations (**2·Cu**, 6 mg L⁻¹; **3·Cu**, 7 mg mL⁻¹; **4·Cu**, 8 mg mL⁻¹) in $\text{CHCl}_3/\text{CHCl}_2\text{CH}_2\text{Cl}$ (4/1, v/v) were first prepared. The solutions were filtered through a 0.45 μm microfilter before use. Then, 60 μL solutions were spin-coated for 60 s on electronic grade glass (15 x 15 mm²) at different speeds (**2·Cu**, 3000 r min⁻¹; **3·Cu**, 3500 r min⁻¹; **4·Cu**, 3000 r min⁻¹) to give a thin film followed by thermal treatment at 70 °C in vacuo. The thicknesses of the films are about 110 nm. Finally, Au (100 nm) was deposited on film in a vacuum chamber at a pressure lower than 6×10^{-4} Pa.

3. Elemental analyses of complexes

Table S1. Elemental analyses of complexes **1·Cu-6·Cu**^{a)}

Complex	Experimental (wt%)			Theoretical (wt%)		
	C	H	Cu ^{b)}	C	H	Cu ^{b)}
1·Cu	58.4	4.6	24.4	58.9	5.0	24.0
2·Cu	61.2	5.8	22.5	61.5	5.9	21.7
2·Cu ^{c)}	62.2	5.4	21.6	61.5	5.9	21.7
3·Cu	63.5	6.3	20.4	63.6	6.6	19.8
4·Cu	65.9	7.7	17.3	66.9	7.7	16.9
4·Cu ^{o)}	66.1	7.3	17.2	66.9	7.7	16.9
5·Cu	54.2	3.6	33.0	55.5	3.6	32.7
6·Cu	56.7	4.4	31.9	57.5	4.4	30.4

^{a)}Prepared in CHCl_3 , unless otherwise specified.

^{b)}Determined by inductively coupled plasma atomic emission spectroscopy.

^{o)}Prepared in DMF.

4. IR spectra of complexes and ligands

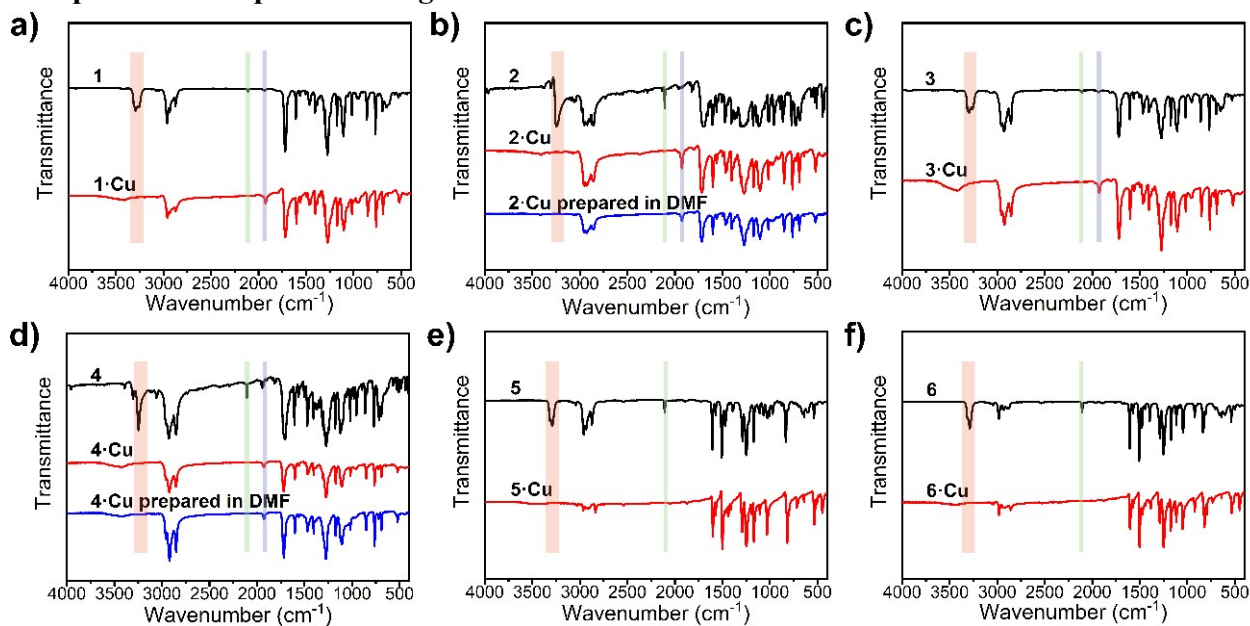


Fig. S1 IR spectra of ligands 1-6 and complexes 1·Cu-6·Cu. The complexes are prepared in CHCl₃ unless otherwise specified.

5. XPS spectra of insoluble complexes

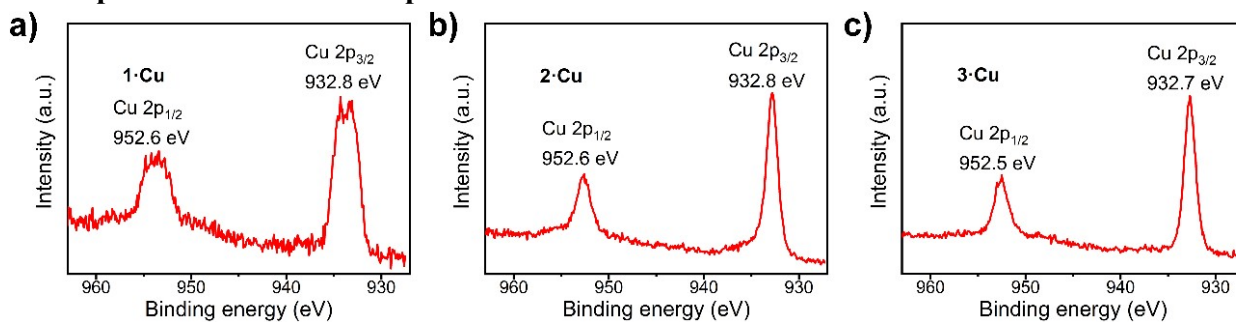


Fig. S2 XPS spectra of insoluble complexes 1·Cu-3·Cu.

6. Raman spectra of insoluble complexes

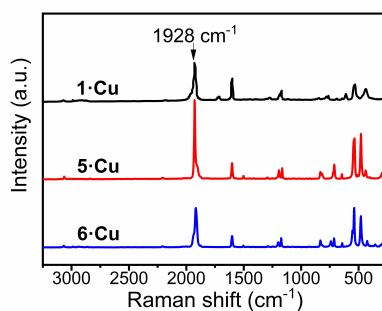


Fig. S3 Raman spectra of insoluble complexes 1·Cu, 5·Cu-6·Cu.

7. Tyndall effects of polymer solutions

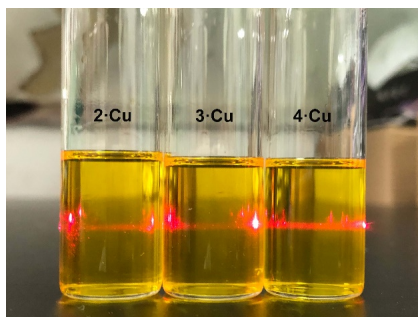


Fig. S4 The photo images of polymer solutions in CHCl_3 under a laser irradiation.

8. Thermogravimetric and differential scanning calorimetry analyses of soluble complexes

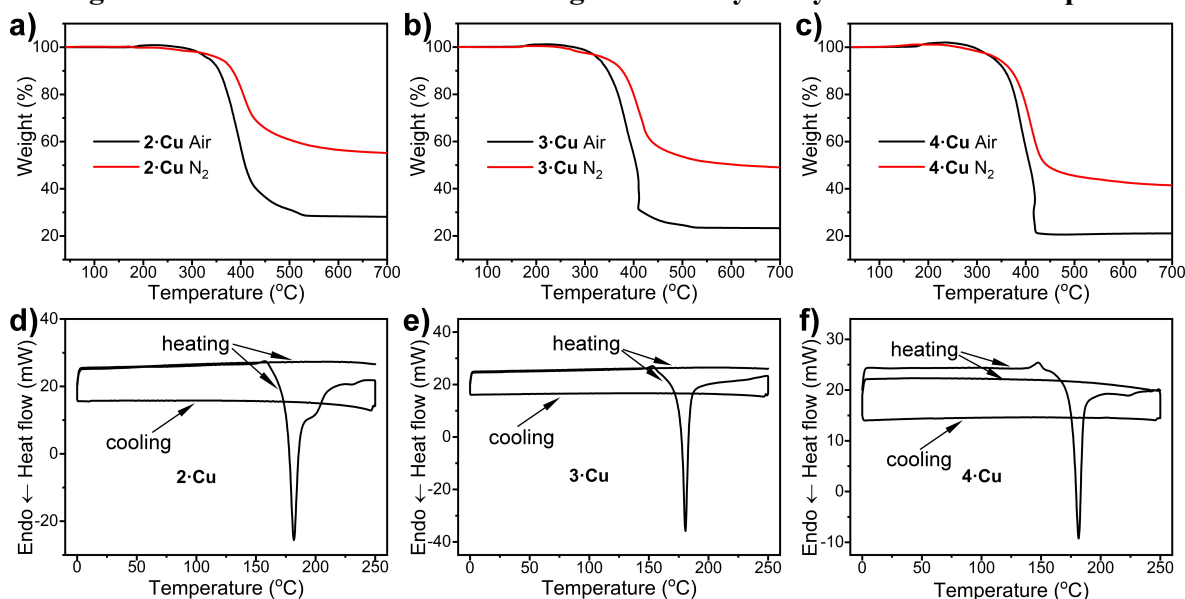


Fig. S5 Thermogravimetric (a-c) and differential scanning calorimetry (d-f) curves of soluble complexes **2-Cu-4-Cu**. DSC scanning temperature: $0\text{ }^{\circ}\text{C} \rightarrow 250\text{ }^{\circ}\text{C} \rightarrow 0\text{ }^{\circ}\text{C} \rightarrow 250\text{ }^{\circ}\text{C}$.

In the second heating process of $0\text{ }^{\circ}\text{C} \rightarrow 250\text{ }^{\circ}\text{C}$, the DSC curves were almost flat. This meant that these samples were irreversible changed in the first heating process. In fact, many indistinguishable species were observed after the samples were kept for 30 min at $150\text{ }^{\circ}\text{C}$ under inert atmosphere.

9. The ESP charge distribution of two acetylides

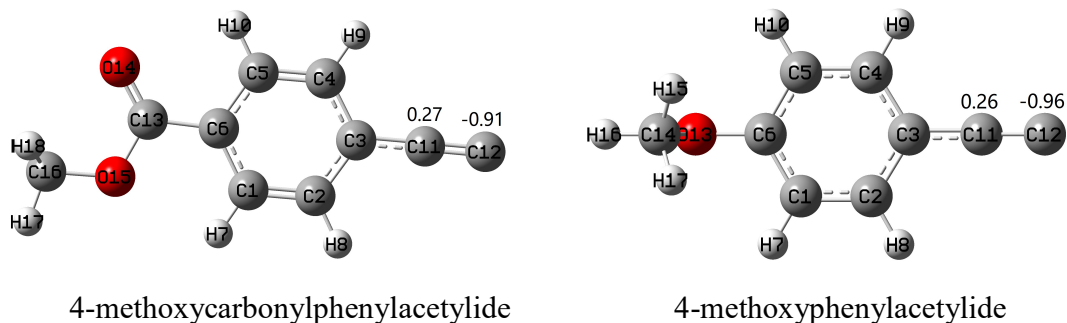


Fig. S6 The ESP charge distribution of two acetylides based on DFT computation

10. UV-Vis absorption spectra of soluble complexes

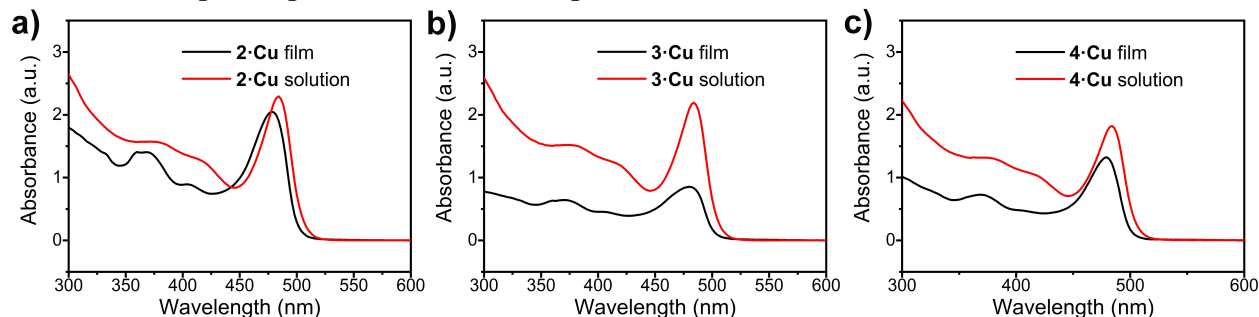


Fig. S7 UV-Vis absorption spectra of films (on quartz plate) and solutions ($c = 0.1 \text{ mg mL}^{-1}$, CHCl_3) of soluble complexes **2-Cu-4-Cu**.

11. Cyclic voltammetry test of soluble complexes

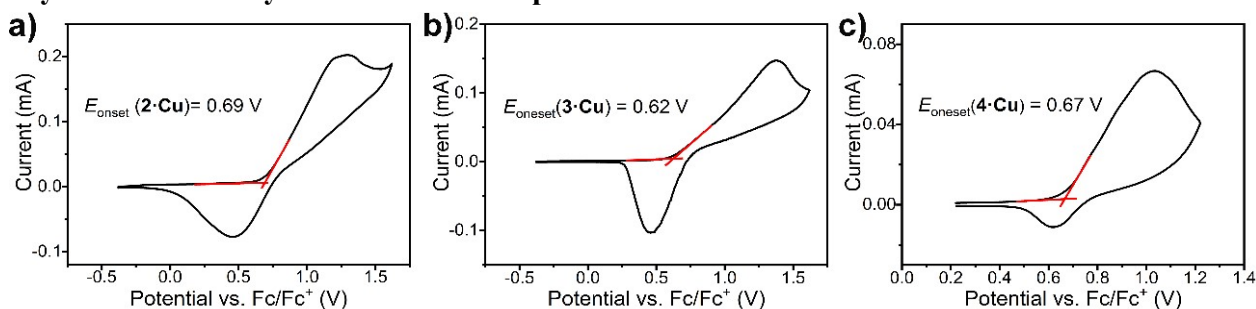


Fig. S8 Cyclic voltammetry curves of soluble complexes **2-Cu-4-Cu** in acetonitrile (0.1 M Bu_4NClO_4) under N_2 atmosphere at a scan rate of 0.05 V s^{-1} . HOMO = $-(E_{\text{onset}} + 4.8) \text{ eV}$; LUMO = HOMO + E_g

12. Excitation and emission spectra of complexes in solution and solid

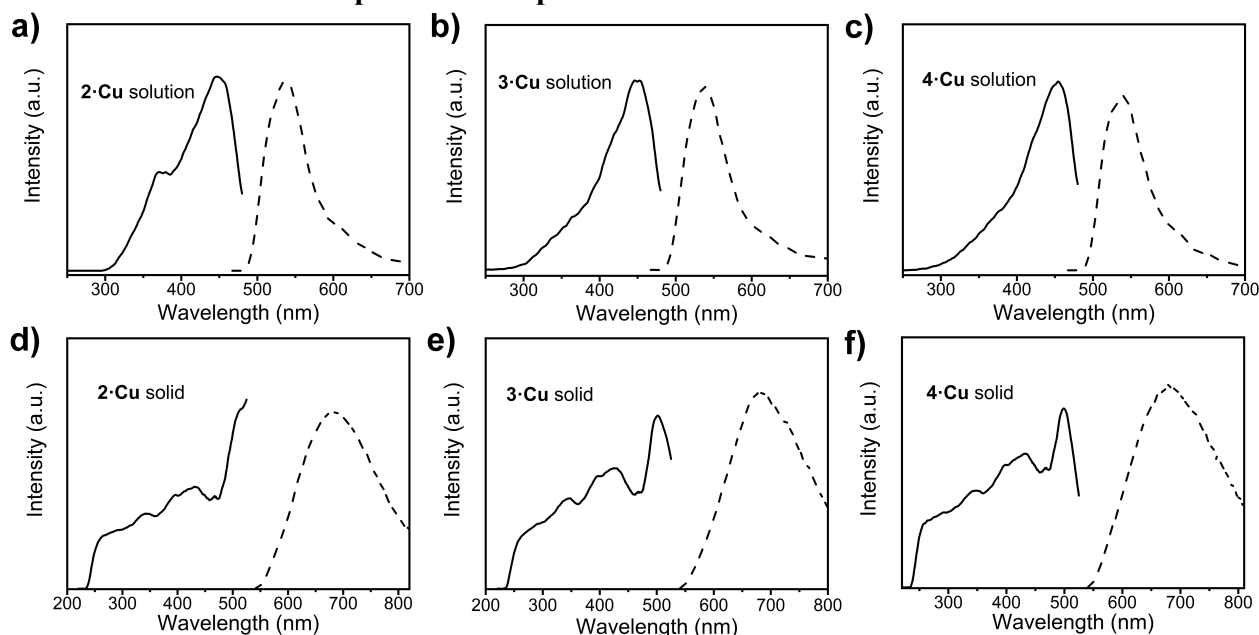


Fig. S9 Excitation (solid line) and emission (dash line) spectra of complexes in CHCl_3 ($c = 0.1 \text{ mg mL}^{-1}$, $\lambda_{\text{ex}} = 447 \text{ nm}$) (a-c) and in solid ($\lambda_{\text{ex}} = 500 \text{ nm}$) (d-f).

13. Time-resolved transient fluorescence decay spectra of complexes

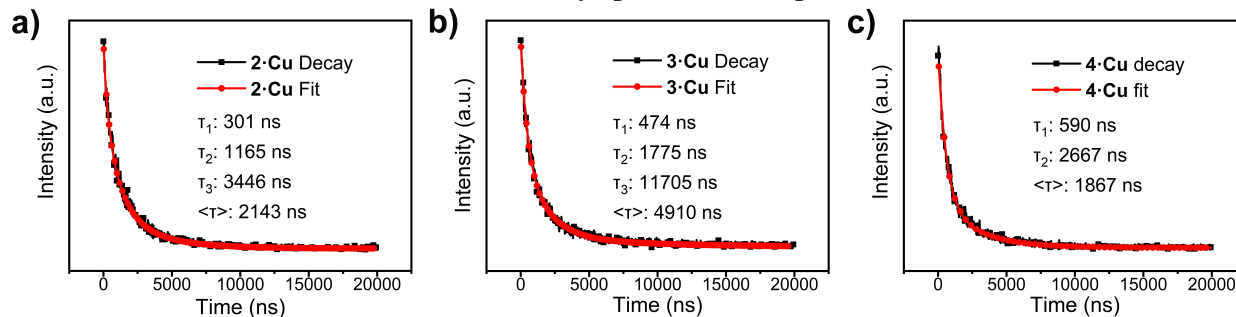


Fig. S10 Room temperature time-resolved transient photoluminescence spectroscopy and fitting profile of soluble complex **2-Cu-4-Cu** monitored at 685 nm ($\lambda_{\text{ex}} = 500$ nm).

14. SEM and TEM images of soluble complexes

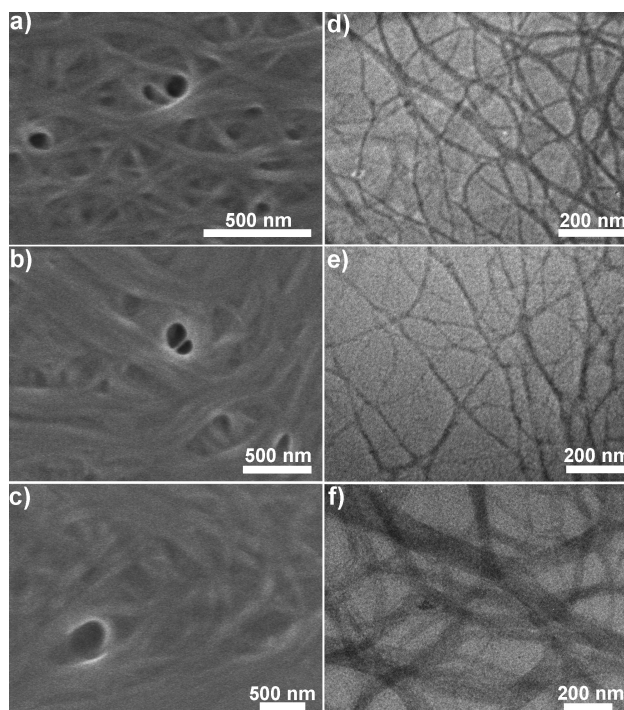


Fig. S11 SEM (a-c) and TEM (d-f) images of soluble complexes **2-Cu-4-Cu**. Scale bars: a-c, 500 nm; d-f, 200 nm.

14. PXRD patterns of complex samples by slow evaporation of CHCl_3 solutions

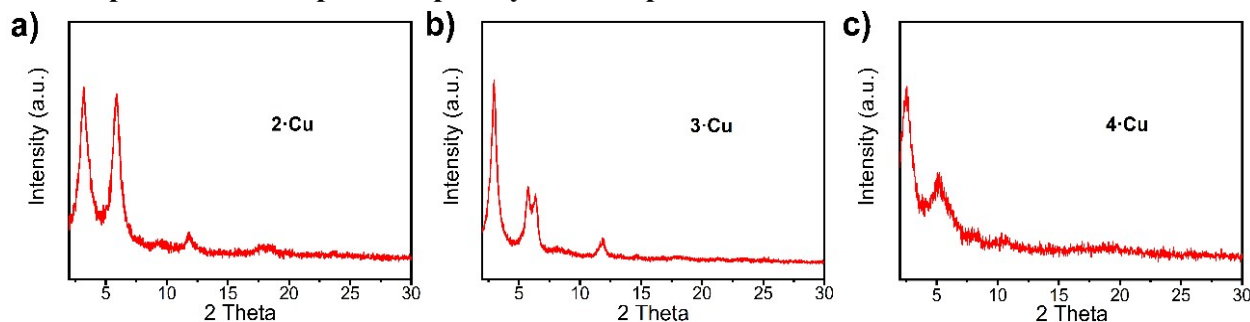


Fig. S12 Powder X-ray diffraction patterns of solid samples **2-Cu-4-Cu** by slow evaporation of complex solutions in CHCl_3 .

15. The photoconductive properties of soluble complexes

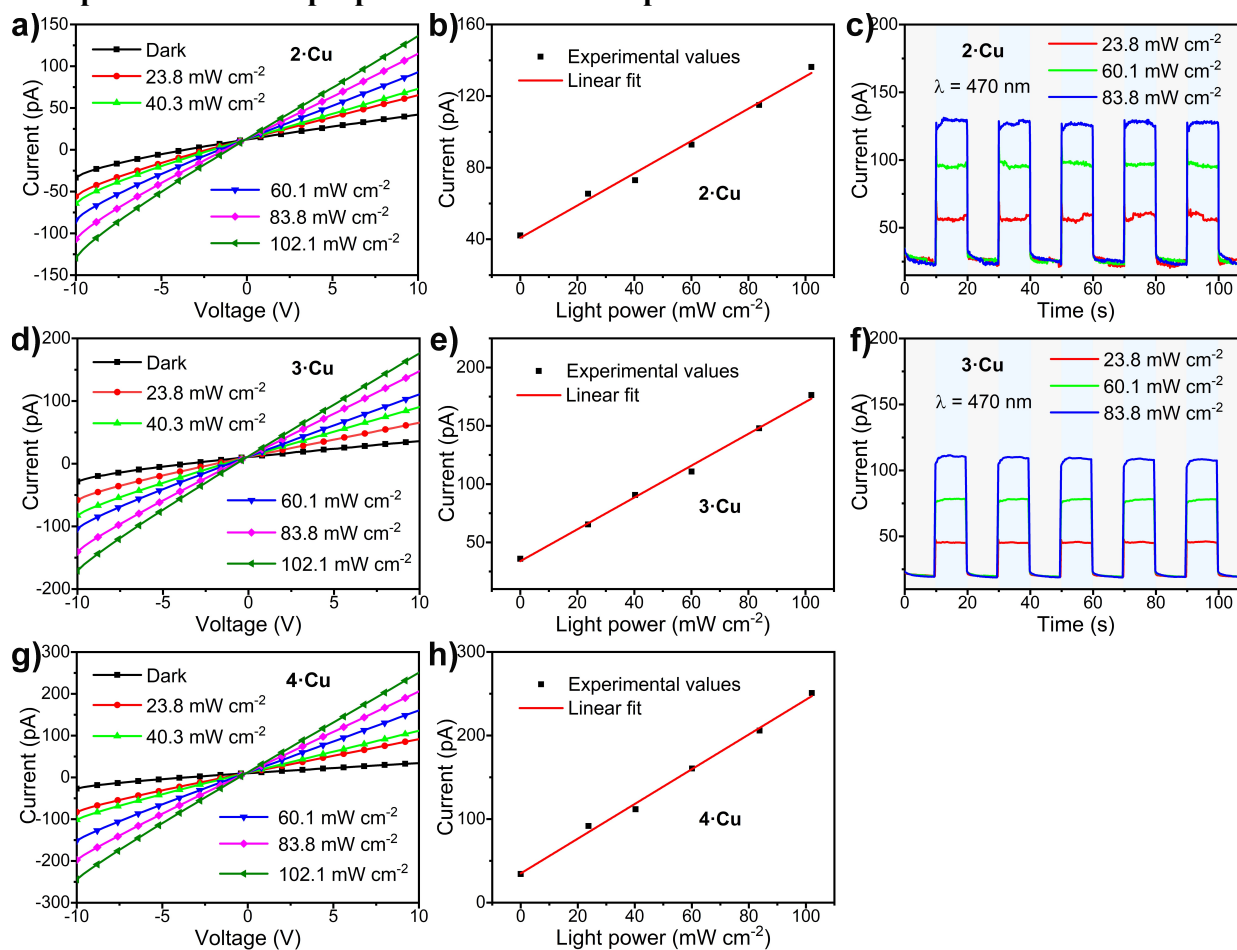


Fig. S13 Photoconductive properties of soluble complexes **2-Cu-4-Cu**. I-V curves of complex film devices measured at room temperature in dark and under illumination with 470 nm light of different intensities (a, d, g); Current-light power curves of complexes film devices at the drain voltage of 10 V (b, e, h); Time-resolved responses of the complex film devices under alternating dark and light illumination (470 nm) (c, f).

References

1. S. S. Y. Chui, M. F. Y. Ng, C.-M. Che, *Chem. Eur. J.*, 2005, **11**, 1739-1749.
2. R. Vadnais, M. A. Beaudoin, A. Beaudoin, B. Heinrich, A. Soldera, *Liq. Cryst.*, 2008, **35**, 357-364.
3. J.-D. Chai, M. Head-Gordon, *Phys. Chem. Chem. Phys.* 2008, **10**, 6615-6620.
4. Gaussian16 v. Revision C.01 (M. J. Frisch, G. W. Trucks, H. B. Schlegel, G. E. Scuseria, M. A. Robb, J. R. Cheeseman, G. Scalmani, V. Barone, G. A. Petersson, H. Nakatsuji, X. Li, M. Caricato, A. V. Marenich, J. Bloino, B. G. Janesko, R. Gomperts, B. Mennucci, H. P. Hratchian, J. V. Ortiz, A. F. Izmaylov, J. L. Sonnenberg, D. Williams-Young, F. Ding, F. Lipparini, F. Egidi, J. Goings, B. Peng, A. Petrone, T. Henderson, D. Ranasinghe, V. G. Zakrzewski, J. Gao, N. Rega, G. Zheng, W. Liang, M. Hada, M. Ehara, K. Toyota, R. Fukuda, J. Hasegawa, M. Ishida, T. Nakajima, Y. Honda, O. Kitao, H. Nakai, T. Vreven, K. Throssell, J. A. Montgomery, Jr., J. E. Peralta, F. Ogliaro, M. J. Bearpark, J. J. Heyd, E. N. Brothers, K. N. Kudin, V. N. Staroverov, T. A. Keith, R. Kobayashi, J. Normand, K. Raghavachari, A. P. Rendell, J. C. Burant, S. S. Iyengar, J. Tomasi, M. Cossi, J. M. Millam, M. Klene, C. Adamo, R. Cammi, J. W. Ochterski, R. L. Martin, K. Morokuma, O. Farkas, J. B. Foresman, and D. J. Fox, , Gaussian, Inc., Wallingford CT, 2019).
5. V. Barone, M. Cossi, *J. Phys. Chem. A*, 1998, **102**, 1995-2001.
6. M. Cossi, N. Rega, G. Scalmani, V. Barone, *J. Comput. Chem.*, 2003 **24**, 669-681.
7. U. C. Singh, P. A. Kollman, *J. Comput. Chem.*, 1984, **5**, 129-145.
8. B. H. Besler, K. M. Merz Jr, P. A. Kollman, *J. Comput. Chem.*, 1990, **11**, 431-439.
9. J. S. Bang, Y. J. Kim, J. Song, J. S. Yoo, S. Lee, M. J. Lee, H. Min, K. W. Hwang, K. H. Min, *Bioorg. Med. Chem.*, 2012, **20**, 5262-5268.